

## Aerial Infrared Surveys of Reykjanes and Torfajökull Thermal Areas, Iceland, with a Section on Cost of Exploration Surveys

G. PÁLMASSON \*, J. D. FRIEDMAN \*\*, R. S. WILLIAMS Jr. \*\*\*, J. JÓNSSON \* AND K. SAEMUNDSSON \*

### ABSTRACT

In 1966 and 1968 aerial infrared surveys were conducted over 10 of 13 high-temperature thermal areas in Iceland. The surveys were made with an airborne scanner system, utilizing radiation in the 4.5-5.5  $\mu\text{m}$  wavelength band.

Supplementary ground geological studies were made in the Reykjanes and Torfajökull thermal areas to interpret features depicted on the infrared imagery and to relate zones of high heat flux to tectonic structure. In the Reykjanes area in southwestern Iceland a shallow ground temperature map was prepared for temperatures at a depth of 0.5 meters; comparison of this map with the infrared imagery reveals some striking similarities.

It appears that aerial infrared surveys outline the surface thermal patterns of high-temperature areas and aid in relating these patterns to possible geological structures controlling the upflow of hot water. Amplitude-slicing techniques applied to the magnetically taped airborne scanner data permit an estimate to be made of the natural heat output on the basis of size of area and specific radiance.

In addition to their value in preliminary studies of high-temperature areas, infrared surveys conducted at regular intervals over thermal area under exploitation can provide valuable data on changes that occur in surface manifestations with time.

### Introduction

In the summers of 1966 and 1968 airborne infrared surveys were undertaken over several high-temperature areas in Iceland as a cooperative project between the U.S. Geological Survey, the U.S. Air Force Cambridge Research Laboratories, the University of Michigan and the Icelandic National Energy Authority. The purpose was to test the usefulness of the infrared technique over thermal areas in various stages of exploration. At the same time surveys were made over several active volcanoes in Iceland, but results of these surveys will not be described here.

This report describes the instrumentation used, the results obtained over two selected areas, and discusses infrared surveys in preliminary exploration of thermal areas. A brief discussion on the cost of airborne infrared surveys is also included.

Some aspects of the infrared surveys in Iceland have been discussed elsewhere (FRIEDMAN, WILLIAMS 1968; FRIEDMAN ET AL. 1969).

### Areas surveyed

In the 1966 survey six of the 13 high-temperature areas in Iceland were surveyed, i.e., the Reykjanes,

Krísuvík, Kverkfjöll, Námafjall, Krafla and Theistareykir areas. Surveys were also planned over the remaining areas, but could not be carried out because of adverse weather conditions. In the 1968 survey the Reykjanes and Kverkfjöll areas were resurveyed and two more added, the Hengill and the Torfajökull areas. The location of the survey areas is shown in Figure 1.

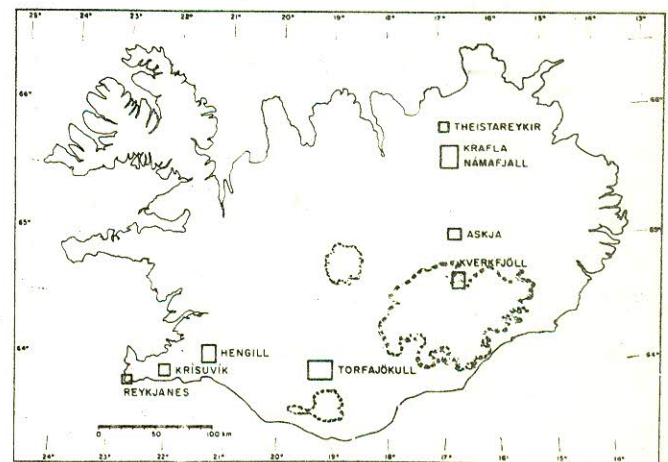


FIG. 1. — Sites of aerial infrared surveys of high-temperature thermal areas in Iceland.

The flight altitudes were generally between 610 and 6100 meters depending on the degree of detail that was desired. The flights were usually carried out in the early morning before sunrise, to avoid as much as possible the disturbing effects of solar radiation.

### Instrumentation and data processing

The optical-mechanical line-scan system used in the aerial infrared surveys of Iceland in August 1966 and August 1968 was designed and constructed by the University of Michigan as a geophysical research instrument. The M1A1 system (Figure 2) utilizes a photo-voltaic indium antimonide solid-state detector sensitive to radiation in the 1.0  $\mu\text{m}$  to 5.5  $\mu\text{m}$  wavelength band and was operated unfiltered over Reykjanes, Torfajökull and other geothermal fields during night surveys when solar irradiation of the earth's surface was at a minimum. Under these conditions blackbody emission from ambient-temperature terrain features and geothermal sources was the dominant thermal radiation from the terrestrial surface, particularly in the 4.5  $\mu\text{m}$  to 5.5  $\mu\text{m}$

\* National Energy Authority, Laugavegur 116, Reykjavík, Iceland.

\*\* U.S. Geological Survey, Washington, D.C. 20242, USA.

\*\*\* Air Force Cambridge Research Laboratories, Bedford, Mass., USA.



band where peak detector response and relatively high blackbody emission partly coincide spectrally with an atmospheric transmission window (Figure 3).

The line-scan system (Figure 2) operates in the following way: the optical elements focus radiation emitted from the earth's surface onto the detector which

transduces the infrared component into wideband electrical signals and provides an input to an image recorder. The video signals from each scan modulate the intensity of a cathode-ray-tube spot as it sweeps across the face of the cathode ray tube. Film moving through a camera focused on the tube is exposed in relation to

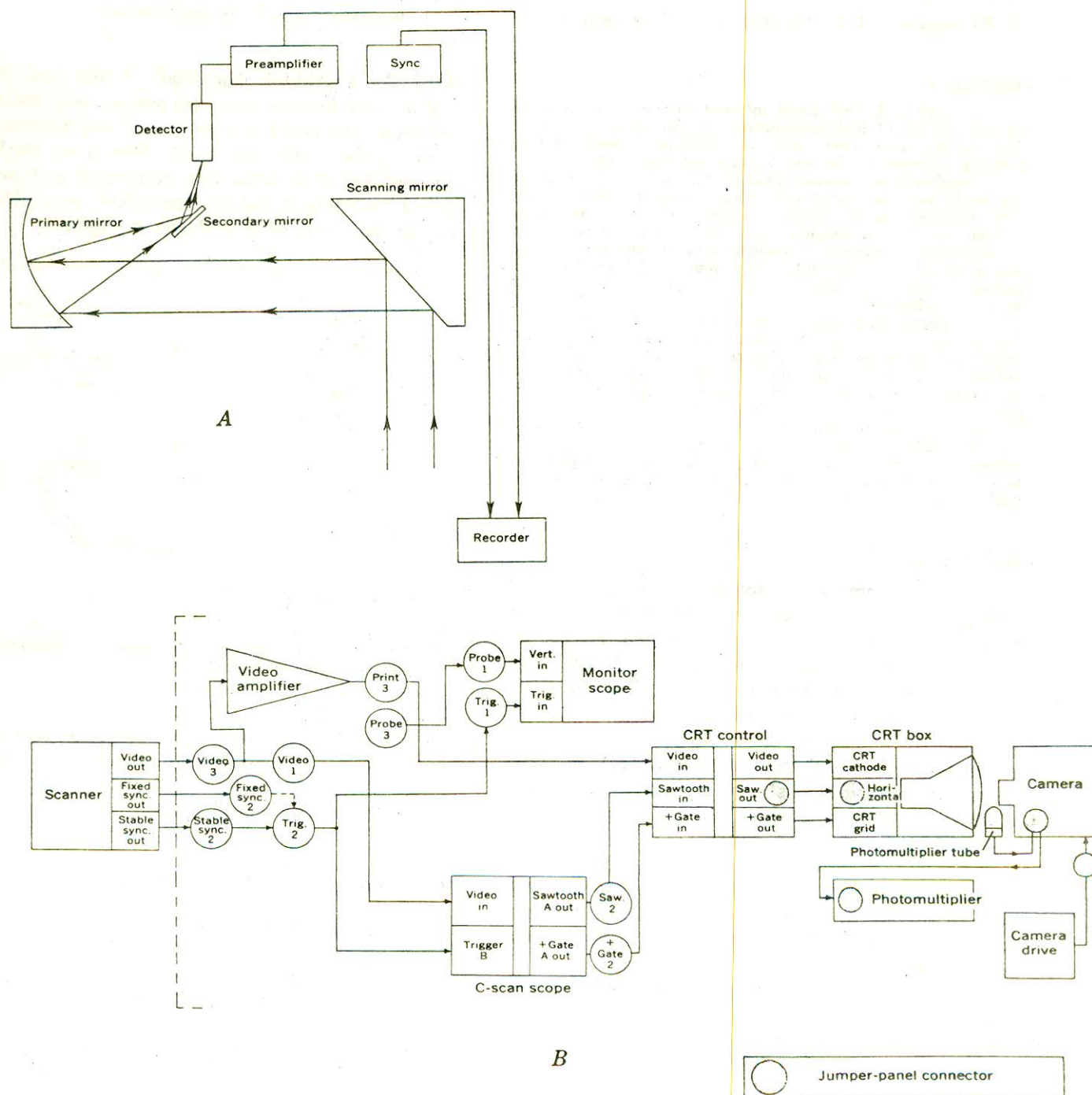


FIG. 2. — Schematic diagram of the MIAI line-scanning system, which electronically records a thermal image of the terrain over which it passes. The scanner can be separated into two major components, the scanning unit, A, and the recording unit, B. The scanning unit utilizes a Newtonian optical system coupled with a four-sided scanning mirror to produce continuous-strip infrared imagery. As shown in B, the infrared scanner provides three basic signals required in recording the data acquired, the video signal and two types of synchronizing pulses. The basic function of the image recording unit is to convert the electronic video amplitude variations from the scanner preamplifier into light variations of relative intensities on an intensity-modulated cathode-ray tube (CRT). The resulting images are then recorded on continuously moving film (from FRIEDMAN ET AL. 1969, p. C92).



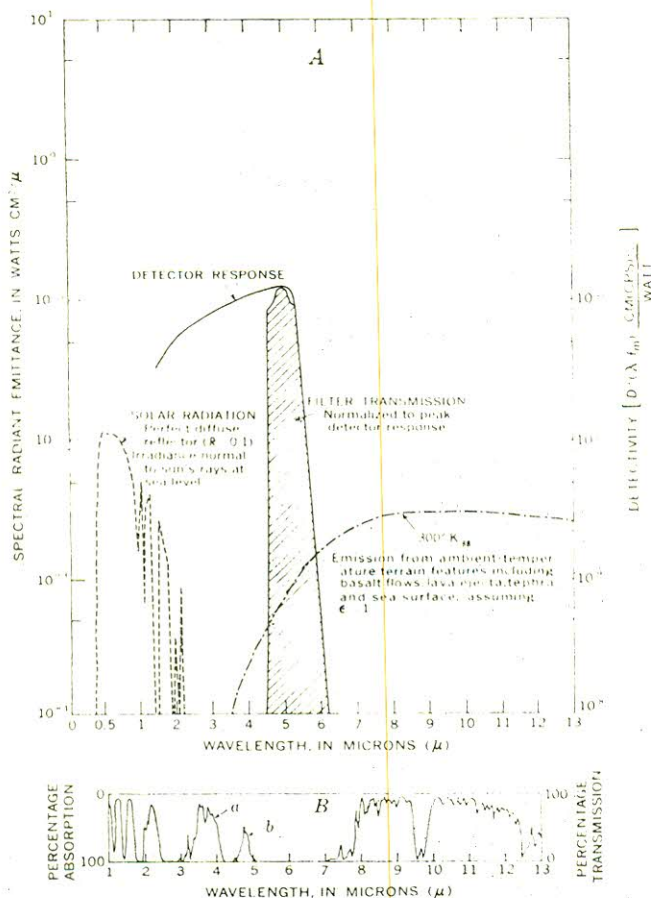


FIG. 3. — A) Estimated radiant emittance from ambient-temperature terrain features including basalt flows, lava ejecta, tephra, and sea surface, assuming an emissivity of unity, based on the Stefan-Boltzmann function. Also shown are spectral solar radiation and the airborne MIAI infrared scanner filter transmission normalized to peak InSb detector response. B) Infrared spectrum of solar irradiation of the earth's surface showing atmospheric transmission windows (a, b) utilized by MIAI airborne scanner over Iceland in 1966 and 1968. (Modified from FRIEDMAN ET AL. 1969, p. 91).

the intensity of the flying spot. The film moves at a rate proportional to the ratio of apparent ground speed to aircraft altitude, thus generating a video image (FRIEDMAN, WILLIAMS, PÁLMASSON, MILLER 1969, p. C91-92). In 1968, a more sophisticated magnetic video tape recording unit was added to the system to supplement the direct-film recording unit.

The magnetic tape recording system made possible an analysis of the data by means of an electronic signal-amplitude slicing technique in preference to the iso-densitracer method (WILLIAMS ET AL. 1968, p. 179, Figures 6 and 9) which is limited by film response shortcomings. A signal recovered directly following the preamplifier does not contain the nonlinearities associated with further amplification and recording in the scanner system. The amplitude of tape recorded signals is proportional to detector output voltage, and the detector is, over a very wide range, a linear transducer from

input flux density to output voltage (ENGLAND, MORGAN 1965, p. 682). In applying the signal amplitude level slicing technique to the video tape records of infrared emission from Iceland in 1968, a threshold circuit, a 1000-division potentiometer, and a solid-state comparator analyzed a 2.5 volt input signal and yielded a series of discrete level samples printed as separate images, each correlative with a thermal emission increment. Composite images made from the full range of signal intensities were also derived from the magnetic tape.

### Objectives of the surveys

In geothermal areas an aerial infrared survey can be expected to furnish useful information that can be related to the heat discharge at the surface. The surveys in Iceland were carried out for the purpose of evaluating the infrared technique as an exploration tool for the mapping of surface thermal anomalies. Quantitative data on which to base such an evaluation have heretofore been scarce. A correlation with surface heat flow, which in turn is related to the shallow temperature field, would provide the most direct approach to the evaluation of the infrared technique.

The high-temperature areas in Iceland are in varying stages of exploration. Some of them have been explored in detail by ground surveys and exploration drilling, whereas others have not been completely explored. One thermal field was selected from each group to make a closer examination of the merits of the infrared surveys.

The Reykjanes area in southwest Iceland was chosen from the first group. This is one of the smallest high-temperature areas in Iceland. It has recently been explored in some detail by surface surveys and drilling (cf. paper by BJÖRNSSON ET AL., this Symp.). A shallow temperature map was made specifically to aid in the interpretation of the infrared imagery.

The Torfajökull area in south-central Iceland was chosen from the other group. This is the largest high-temperature area in Iceland, about 100 km² in size. It has so far been explored only by preliminary geological and geochemical surveys. The possible merits of the infrared technique in a relatively little-explored area should stand out clearly here.

### The Reykjanes area

The geology of the Reykjanes area is described in some detail by BJÖRNSSON ET AL., (this Symp.). The area is at the southwestern tip of Iceland, where the crest of the submarine Reykjanes Ridge becomes subaerial. It is completely covered with post-glacial lava flows, pillow lavas and palagonite breccias, presumably formed subglacially during the last glaciation, but which may have been formed by submarine eruptions (Figure 4). The lavas were erupted from several fissures and shield



volcanoes. The most characteristic features of the area are the many faults and tectonic fissures trending north east-southwest. Vertical displacements of up to 12 meters are visible on the main faults. Almost the only non-indurated material covering the area is clay in and around the thermal areas. Vegetation is very sparse except near the thermal area and the nearby Reykjanes lighthouse. The dominant plant in the lava field is moss (*Racomitrium lanuginosum*). The thermal activity is closely associated with tectonic fractures, and covers an area of approximately 1 km<sup>2</sup>. That is characterized by many steam vents and mud pools. Only three hot-water springs are found in the area, two of them with highly saline water. Earthquakes occur frequently and have sometimes caused changes in the surface manifestations of thermal activity. The most recent earthquake (magnitude 4.1) was in October 1967.

A temperature survey at a depth of 0.5 m was carried out on a grid traverse system over the whole area (Figure 5) as a basis for a quantitative evaluation of the thermal anomalies on the imagery. A fairly sharp distinction was noted between areas with temperatures less than about 40 °C at 0.5-meter depth and areas with

temperatures of over 80 °C. At the boundary between these temperature zones the temperature changes fairly rapidly in horizontal directions. This transition zone probably marks the boundary of areas with predominantly convective heat flow.

Detailed studies of the near-surface heat transport mechanism have been made at Wairakei, New Zealand (ROBERTSON, DAWSON 1964; DAWSON 1964). They find that conduction is the predominant mechanism of heat transfer until the difference between the temperatures at the surface and at a depth of 1 meter reaches a value of about 25 °C. They have furthermore studied the shallow temperature field in relation to heat flow values. On the assumption that near-surface heat transport conditions are similar in the Reykjanes field to conditions at Wairakei, it is possible to relate the shallow-temperature measurements to the heat flow and thus by a comparison with the infrared imagery obtain a semi-quantitative estimate of the minimum heat flux that can be detected with some confidence on the infrared imagery.

In a similar study in the Yellowstone National Park WHITE and MILLER (1969) used individual snowfalls

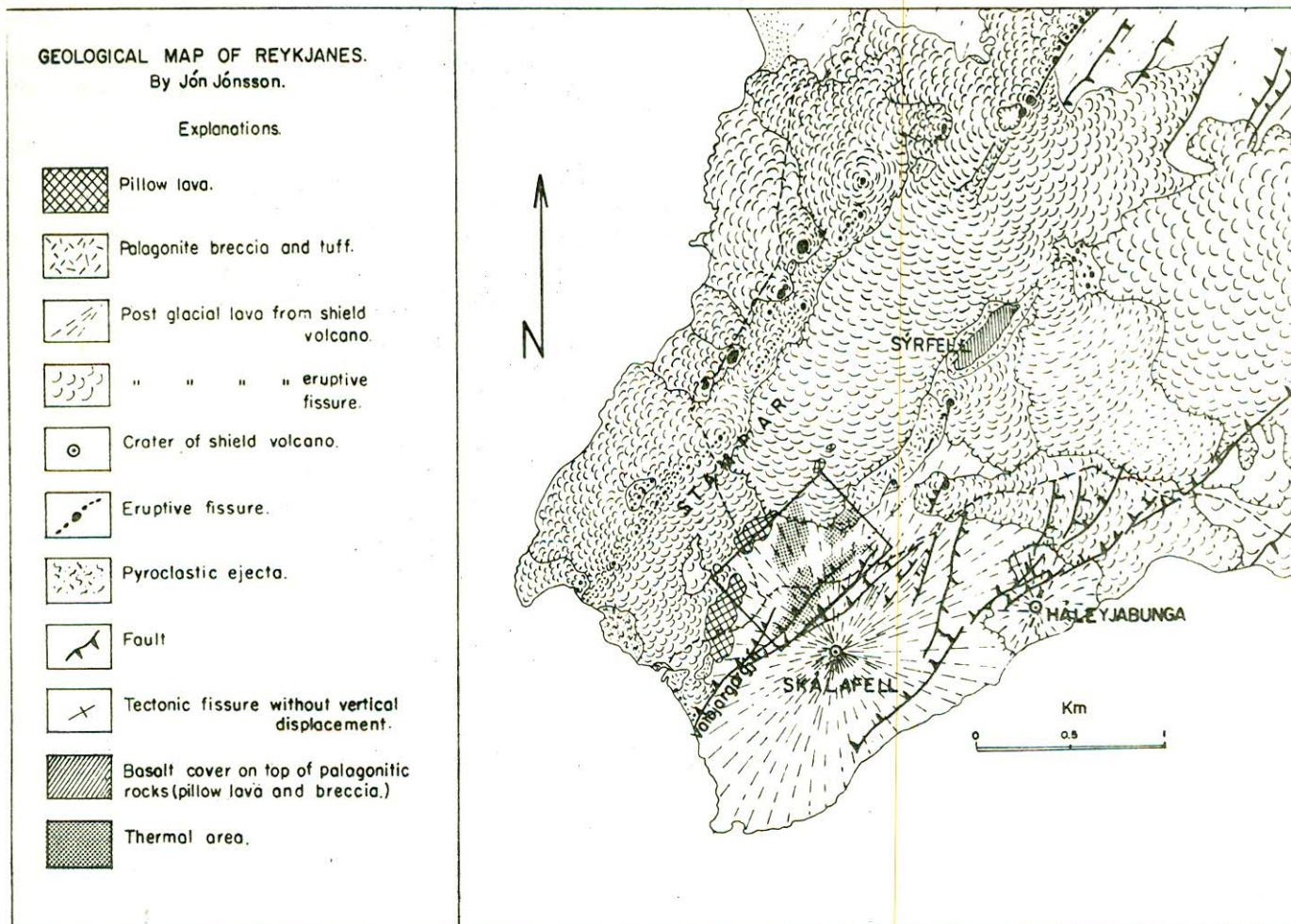


FIG. 4. — Geological map of the Reykjanes thermal area.



as calorimeters. The lowest heat flows that they could detect are in the range 150-500  $\mu\text{cal}/\text{cm}^2 \text{ sec}$ .

1966 and 1968 aerial night images of the Reykjanes geothermal area are shown in Figures 6a and 6b.

The 1968 imagery of the Reykjanes area was processed by the amplitude slicing technique to give separate images, each corresponding to a cutoff of signals below a certain level. The series of images so obtained is shown in Figure 6c-6h. The last image shows only the strongest anomalies, whereas the composite image of 1968 is the most sensitive and shows tonal contrasts produced by differential heating by the sun and by differences in vegetation. These weaker anomalies are already completely cut out in the second image.

By comparing the most sensitive image with the temperatures at 0.5 meter depth it is possible to make some inferences about the sensitivity of the infrared imagery to abnormal heat flows. In Figure 6i a few selected areas which stand out clearly on the imagery have been traced and marked by numbers. The following temperature observations have been made in these areas.

In areas 1, 5 and 6 the temperature at 0.5 meter depth is 60-70°C. Vegetation is scanty and the stony soil cover is mostly 50-60 cm thick. Some small steam

vents occur along a tectonic fracture. The areas 2,3 and 4 are similar but with higher temperatures of 85-90°C. Area 7 is covered with grass and the temperature is 85-95°C. In area 8 the hydrothermal clay is covered with 15-20 cm of loessial soil and with relatively dense grass vegetation. The temperature at 0.5 meter depth is 30-50°C. Area 9 is hydrothermal clay without vegetation. Many steam vents and mud pools are within this area. The temperature is 95-100°C. Area 11 is a hot-water spring, formed in 1968, with a surface temperature of 100°C. Area 12 is also a hot-water spring with highly saline water at 100°C. Area 13 is a hot-water spring formed in 1967 and is at 98°C. Area 14 is a mud pool or more exactly a group of mud pools with temperatures of 95-100°C. Another group of mud pools near to it forms a rough ring pattern which does not show on conventional aerial photographs. Perhaps there are some ring structures (volcanic pipes?) in this place, hidden by more recent lava flows.

On the basis of the shallow-temperature map and the above observations we conclude that an anomalous heat flow can be recognized on the imagery with some confidence if the temperature at a depth of 0.5 m is about 50°-70°C. This is well within the range of convection as the pre-dominant mechanism of heat transfer. Because

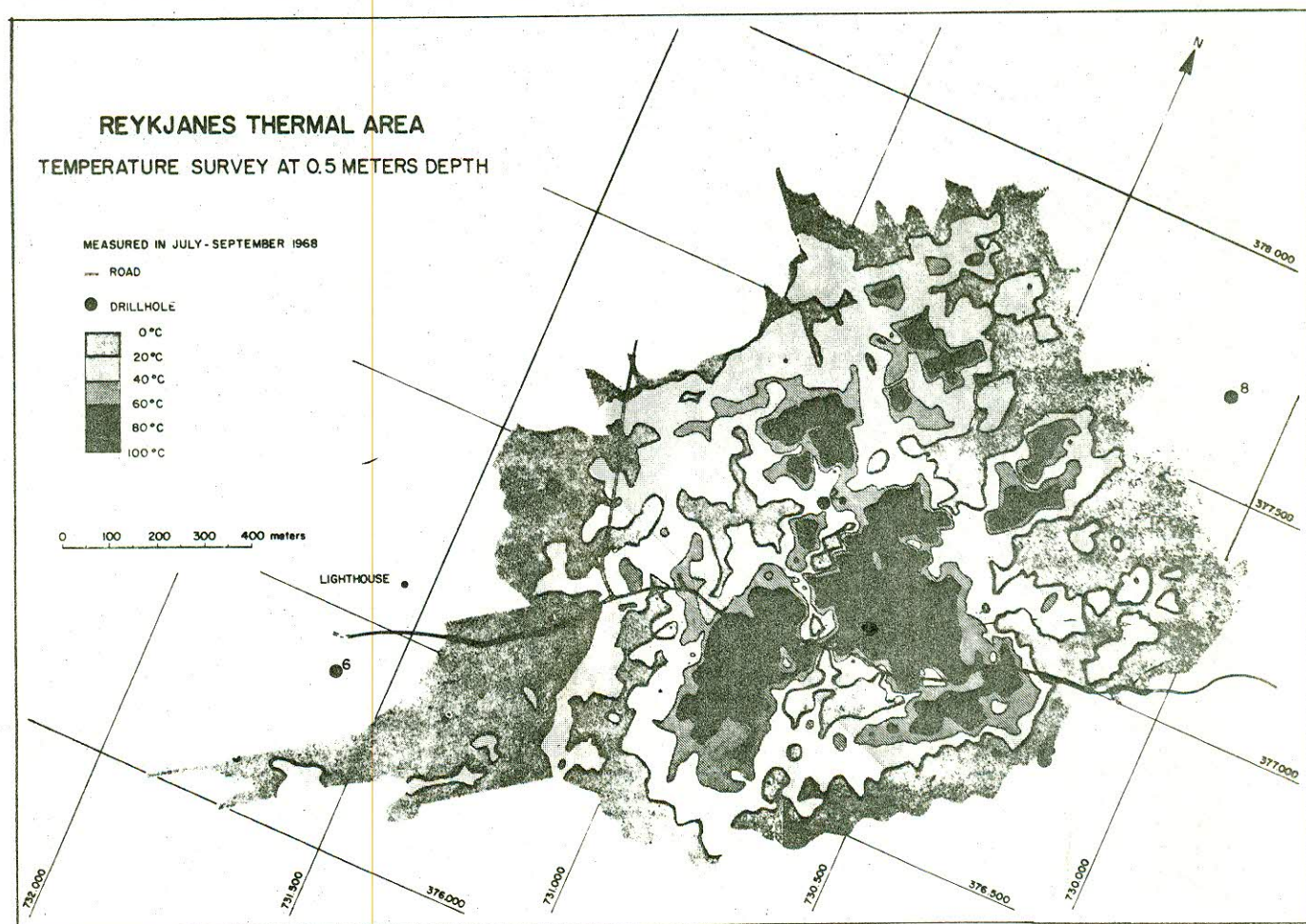


FIG. 5. — A shallow temperature map of the Reykjanes thermal area.



of the dominance of convective heat flow at both Wai-rakei and Reykjanes (where the heat flux is 2 to 3 orders of magnitude greater than the normal conductive heat flux of the earth), it is assumed that differences in thermal conductivity of surface materials in these two geothermal areas are of little importance in affecting total heat flow. Using the data of DAWSON (1964) and ROBERTSON and DAWSON (1964) we calculate that the temperatures of 50°-70°C at 0.5 meter depth correspond

to heat flow values of 2-7 cal/m<sup>2</sup> sec, or 200-700  $\mu$ cal/cm<sup>2</sup> sec. This is in very good agreement with the results of WHITE and MILLER quoted above.

This corresponds roughly to 100-500 times the normal heat flow, but heat flow values of 5-10 times the normal value may be significant in geothermal exploration. Thus the IR technique is not very efficient for detecting *weak* heat flow anomalies because of background noise, caused by differences in emissivities of various kinds of surface materials. The relation between minimum detectable heat flow by an airborne infrared scanner utilizing an InSb detector and mean heat flow density of some typical geothermal areas is given in Table 1.

A study of the minimum detectable radiant flux over the volcano Surtsey, on the basis of data from WILLIAMS ET AL. (1968), indicates that the minimum detectable difference in radiant flux above the geologic « noise » level is about 0.7 cal/m<sup>2</sup> sec. According to DECKER and PECK (1967) the heat loss by surface radiation from the Alae lava lake, Hawaii, was about 10 percent of the total heat loss. If the surface radiation



FIG. 6a. — Aerial infrared (4.5.5  $\mu$ m) night image of the Reykjanes geothermal area, August 20, 1966.

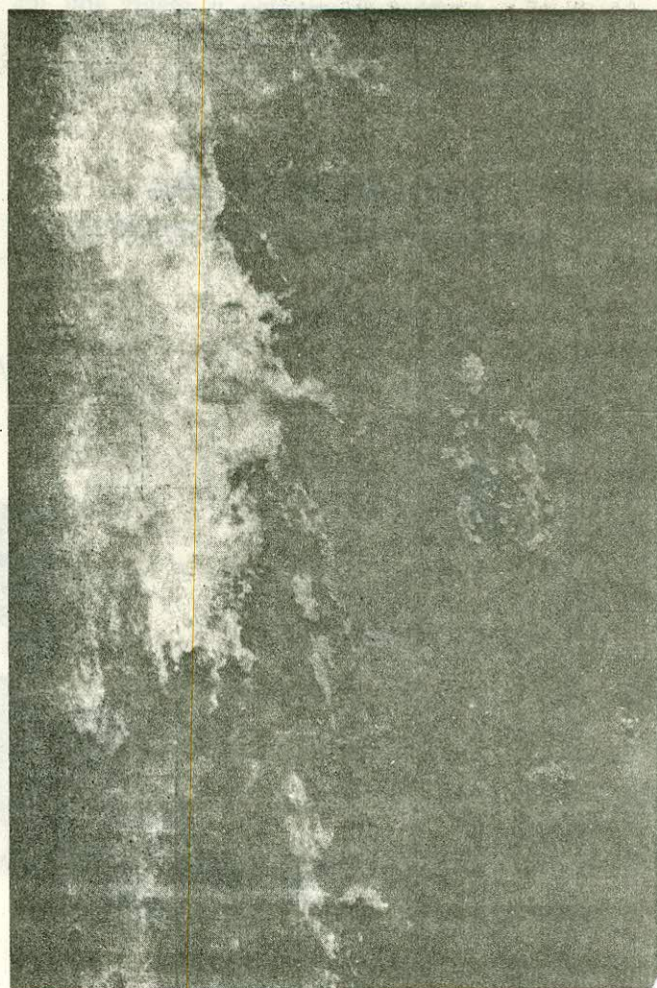


FIG. 6b. — Aerial infrared (4.5.5  $\mu$ m) night image of the Reykjanes geothermal area, August 1968.



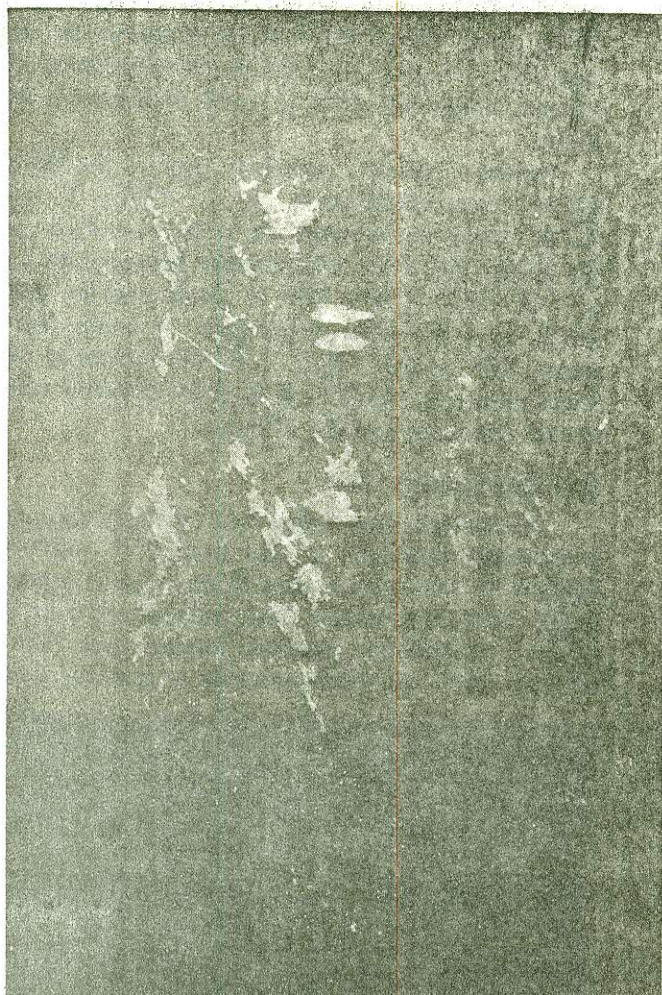


FIG. 6 c. — Signal amplitude level slices constructed from 1968 magnetic videotape record of Reykjanes image (Fig. 6 b). White areas show incremental emission above selected threshold levels.

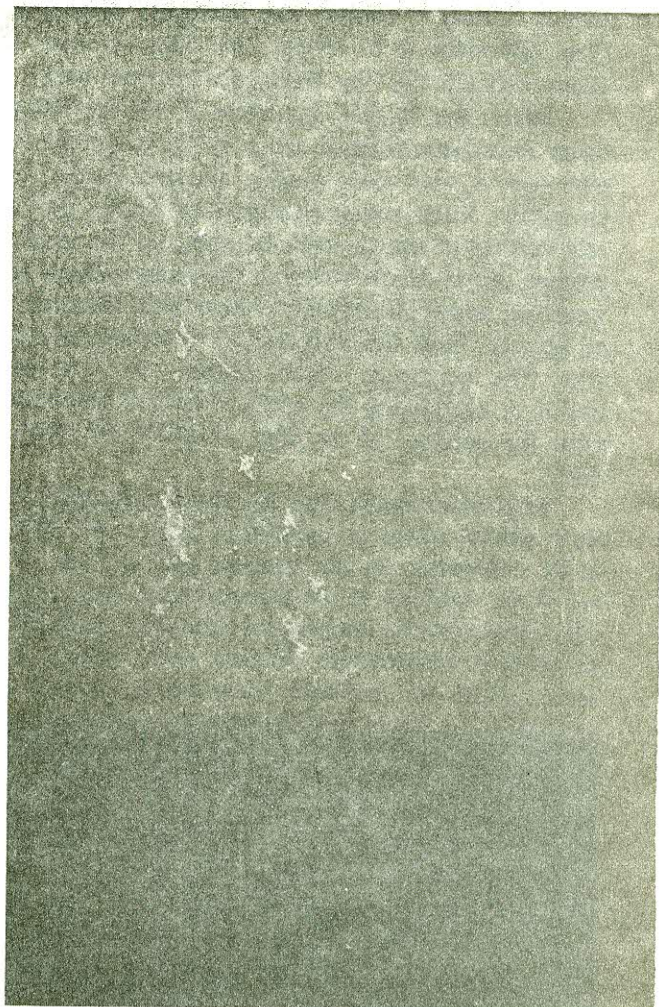


FIG. 6 d. — Signal amplitude level slices constructed from 1968 magnetic videotape record of Reykjanes image (Fig. 6 b). White areas show incremental emission above selected threshold levels.

TABLE 1. — Mean heat flow density of selected thermal areas compared with level of detectability by aerial infrared scanner, utilizing an indium antimonide detector.

Selected Thermal Regions and Areas		Mean Heat Flow Density	
Minimum detectable by aerial infrared scanner with InSb detector	Normal regional heat flow of the earth <sup>(1)</sup>	0.015	cal/m <sup>2</sup> sec
	Icelandic neovolcanic zone <sup>(2)</sup>	0.045	cal/m <sup>2</sup> sec
	Reykjanes (estimated)	5	cal/m <sup>2</sup> sec
		2-7	cal/m <sup>2</sup> sec
	small pines, manuka and broom	1	cal/m <sup>2</sup> sec
	manuka, broom	10	cal/m <sup>2</sup> sec
	low stunted manuka	30	cal/m <sup>2</sup> sec
	moss, lichens	60	cal/m <sup>2</sup> sec
	moss	100	cal/m <sup>2</sup> sec
	Ground conditions <sup>(3)</sup> associated with different heat flow levels within Wairakei thermal area	200	cal/m <sup>2</sup> sec
	dead wood, algae, soft thermal clay	500	cal/m <sup>2</sup> sec
	bare ground, thermal clay crust	1000	cal/m <sup>2</sup> sec
	bare ground, visible steam	3000	cal/m <sup>2</sup> sec
	bare ground, audible steam vents		

<sup>(1)</sup> LEE, W. H. K. and S. UYEDA, 1965. <sup>(2)</sup> Estimated from data given by BÖDVARSSON, WALKER 1964, p. 285-300. <sup>(3)</sup> DAWSON 1964, p. D162.



loss at Surtsey is similar, the minimum detectable heat flow difference is  $7 \text{ cal/m}^2 \text{ sec}$ . This is close to the above estimate for the Reykjanes thermal area.

When the weaker anomalies in the Reykjanes imagery have been filtered away by the amplitude slicing technique a very clear picture emerges of the stronger anomalies. Their geometrical pattern clearly shows their relationship to the tectonic fractures in the areas. This pattern shows much better on the imagery than on conventional aerial photographs where hydrothermally altered ground, both hot and cool, is recorded in a similar way. The amplitude sliced imagery can thus be very useful in correlating the surface thermal manifestations with the geology of an area, in particular with fault lines.

It is to be noted that the above discussion of heat flow values refers to conditions where the heat flow is by convection in hot ground, soil or clay. If there are water surfaces in the thermal area, these shows up very clearly on the imagery for relatively small increases in surface temperature. Where such known temperature points are available they can be related to the

voltage values on the amplitude sliced imagery, above which lower radiometric surface temperatures are eliminated. This gives a rough linear correlation of the different amplitude slices to cutoff radiometric temperatures.

Figure 7 shows a resistivity map of the Reykjanes thermal area (BJÖRNSSON ET AL. 1970). It outlines the hot zones at a depth of a few hundred meters, and shows that it is a chimney-like feature with a diameter of about 1 km. This is confirmed by drillings, which have proved a temperature of about  $280^\circ\text{C}$  at about 1000 meters depth. Infrared anomalies (Figure 6b-h) mark the position of thermal emission from the top of this chimney-like feature.

#### The Torfajökull area

Torfajökull area refers to a rhyolite complex approximately  $400 \text{ km}^2$  in size located in south-central Iceland. In the western part of this area is located the largest and most intense high-temperature area in the country. Information gathered during short field trips between 1966 and 1968 provided a basis for interpret-

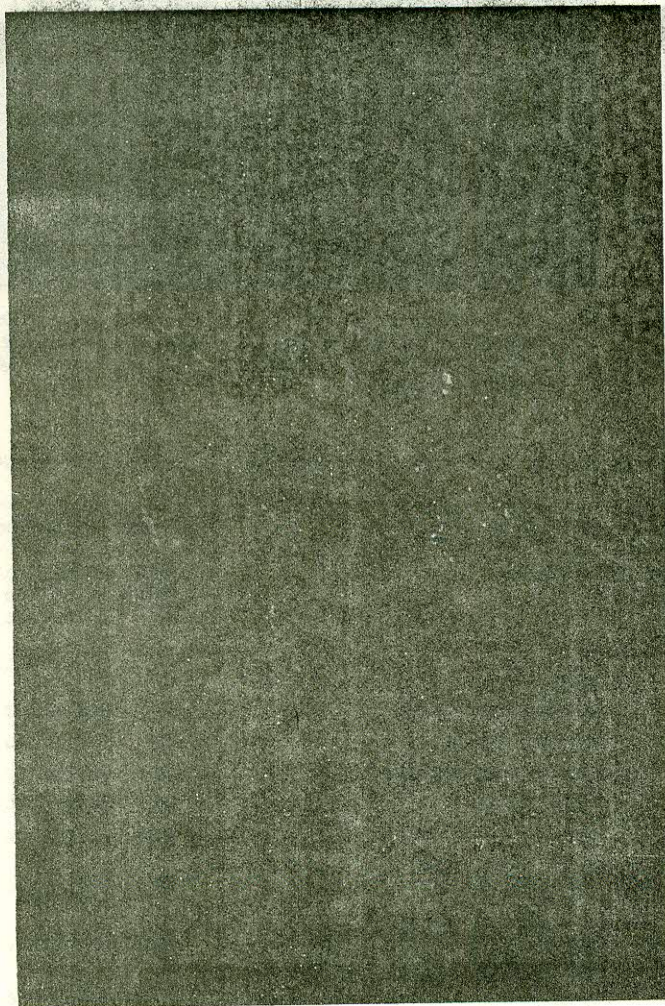


FIG. 6 e. — Signal amplitude level slices constructed from 1968 magnetic videotape record of Reykjanes image (Fig. 6 b). White areas show incremental emission above selected threshold levels.

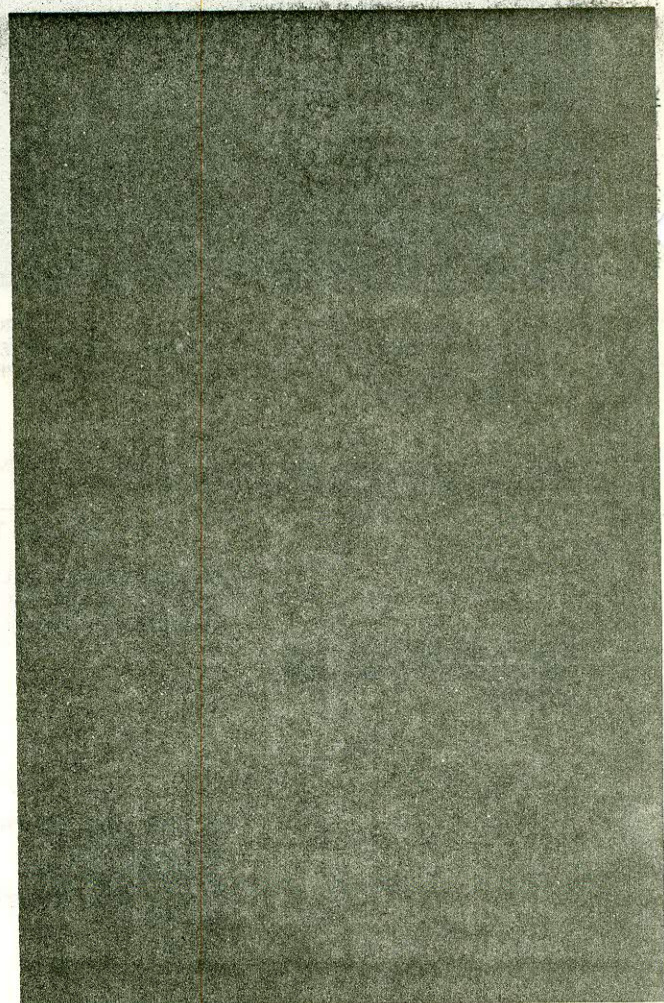


FIG. 6 f. — Signal amplitude level slices constructed from 1968 magnetic videotape record of Reykjanes image (Fig. 6 b). White areas show incremental emission above selected threshold levels.



ing imagery obtained by airborne infrared scanning in August 1968 (SAEMUNDSSON 1969). The infrared imagery consists of 4 strips running almost parallel in an east-northeast direction across the western half of the Torfajökull area (Figure 8). Hydrothermal features are splendidly manifested on the infrared imagery which, in fact, supplied new and valuable information on the distribution of hydrothermal features in this remote and hitherto inadequately known area.

#### OUTLINE OF GEOLOGY

The bedrock of the area consists mainly of three different rock types. These are in order of age from oldest to youngest: rhyolites, hyaloclastites, post-glacial lava flows (Figure 9).

The *rhyolites* are extrusive consisting of many different eruptive units. This rhyolite complex is bounded by abrupt slopes and is 300-400 m higher than the surrounding terrain. Some smaller dome-like or conical hills, the highest more than 200 m, are situated on the rhyolitic plateau. Two sectors have been strongly affected

by erosion, i.e. the area to the south of Laugahraun up to Torfajökull and the area south of Hrafninnusker. There the rhyolitic plateau is deeply cut by numerous ravines and gullies forming a true badland topography. So far, the age of the rhyolites is unknown, but since they underlie the hyaloclastites an age greater than the last glacial stage is almost certain.

The rhyolite complex is bounded on all sides by *hyaloclastites* which form northeast-trending ridge or cone-shaped mountains 100-400 m in height. These rocks invariably overlap the rhyolites at their contacts. The hyaloclastites have been produced by subglacial fissure (ridge) or central (cone) eruptions most probably during the last glacial stage. Locally hyaloclastite eruptions have also occurred within the rhyolite complex. The hyaloclastites are mostly basaltic in composition but andesitic and even rhyolitic varieties are also present.

*Post-glacial lava flows* are widely distributed in depressions and valleys to the north, south and west of the rhyolite complex. Within the complex itself are

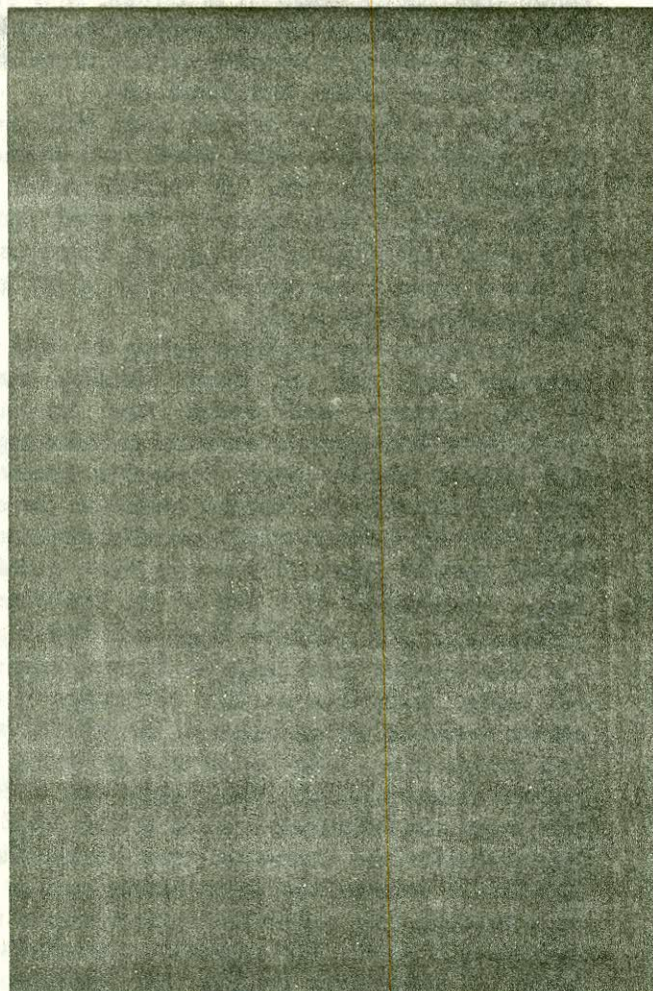


FIG. 6 g. — Signal amplitude level slices constructed from 1968 magnetic videotape record of Reykjanes image (Fig. 6 b). White areas show incremental emission above selected threshold levels.

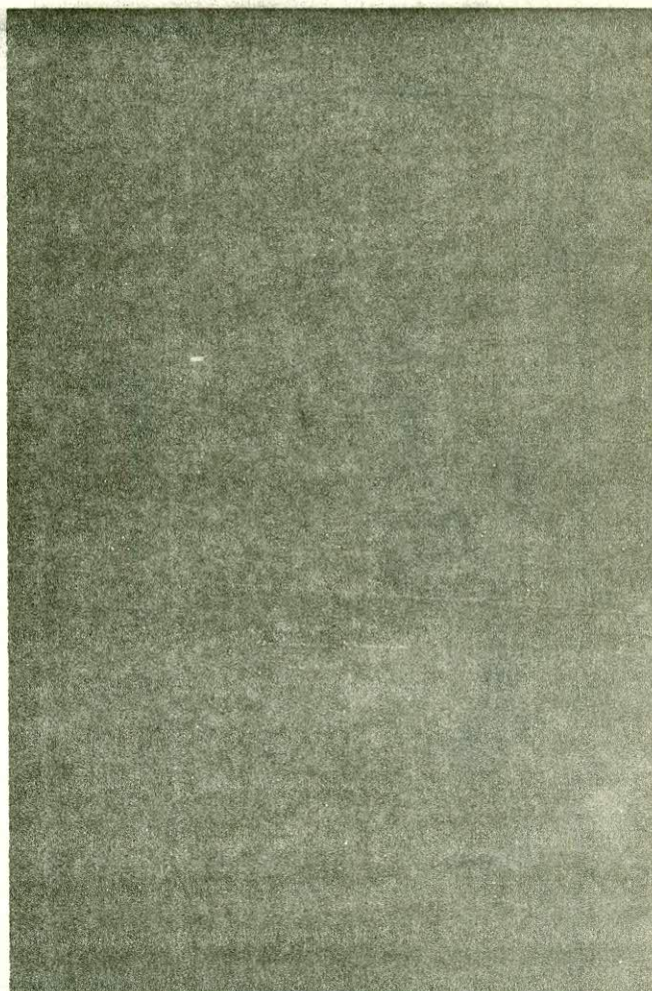


FIG. 6 h. — Signal amplitude level slices constructed from 1968 magnetic videotape record of Reykjanes image (Fig. 6 b). White areas show incremental emission above selected threshold levels.



numerous lavas, most of them rhyolitic in composition.

The bedrock is concealed to a great extent in the Torfajökull area by thick beds of volcanic ash produced by nearby volcanoes and eruption centers within the Torfajökull area itself. Thick fluvial sediments occupy the floors of valleys and depressions within and around the area.

The Torfajökull area may be regarded as a central volcano in an advanced state of development. It is atypical, however, as compared to other known Icelandic central volcanoes as regards the great abundance of rhyolitic rocks. The structure of the area is dominated by two major patterns. A northeast-southwest-trending *regional pattern* represented by numerous eruptive fissures and occasional faults is dominant in the country surrounding the Torfajökull area. This structural pattern continues across the northwestern part of the Torfajökull area itself as is indicated by numerous northeast-trending hyaloclastite ridges and postglacial eruptive centers. Secondly, a *local structural pattern* seemingly related to a collapse caldera is present within the rhyolite complex itself. Numerous arcuate

features are thought to represent this local structural pattern. The hydrothermal features are notably restricted to the proposed caldera, which is over 100 km<sup>2</sup> in size.

#### HYDROTHERMAL FEATURES AS REPRESENTED ON THE INFRARED IMAGERY

The Torfajökull infrared imagery was obtained from 3000 meters altitude at night between 00<sup>27</sup> and 01<sup>35</sup> about 3-1/2 hours after sunset, thus eliminating reflected radiation and recording only emitted infrared radiation. The hydrothermal features show up white against dark grey and grey background on the photographically reproduced imagery strips.

A map of the Torfajökull area (Figure 9) shows the hydrothermal features without distinction as to type according to field data and complementary additions from the infrared imagery marked accordingly. Since the preparation of the map a few of the hot spots revealed by the infrared imagery have been checked in the field and found to be present. Checking of some of the remaining hot spots is necessary before they can be regarded as certain. It is evident from this map that the infrared imagery has contributed greatly in providing a complete picture of the hydrothermal features of the Torfajökull area.

Figure 10 shows an infrared image strip covering the extensive solfatara fields within and around the post-glacial rhyolite lava of Hrafninnusker. The thermal activity is most intense to the south and west of it where individual solfatara groups almost coalesce to form a more or less continuous area of hot ground approximately 2 km<sup>2</sup> in size.

The limited time available during the field reconnaissance trips did not permit detailed mapping of this solfatara area except near its margins where the solfatara groups were less crowded together. The infrared imagery makes it possible, however, to map with precision the solfatara pattern in the central area where the solfatara groups are most numerous and densely crowded. Figure 11 is a map based on infrared-image interpretation of a part of the Hrafninnusker solfatara area on a somewhat larger scale than Figure 9.

The solfatara fields south of Hrafninnusker were not visited in the field so their distribution is almost entirely based on interpretation of the infrared images. It is evident that a major broad zone of intense hydrothermal features extends from a point east of Reykjafjöll across Kaldaklofsfjöll with an arcuate trend up to Hrafninnusker and beyond to Vestur-Reykjadalir. The existence of a deep-seated infrastructure such as a caldera ring fault may explain this marked zone of intense hydrothermal activity. This suggestion was initially based largely on topographic evidence and more geological work is needed to reveal the structural details.

The Vestur-Reykjadalir solfatara group is located in an area characterized by northeast-trending hyaloc-

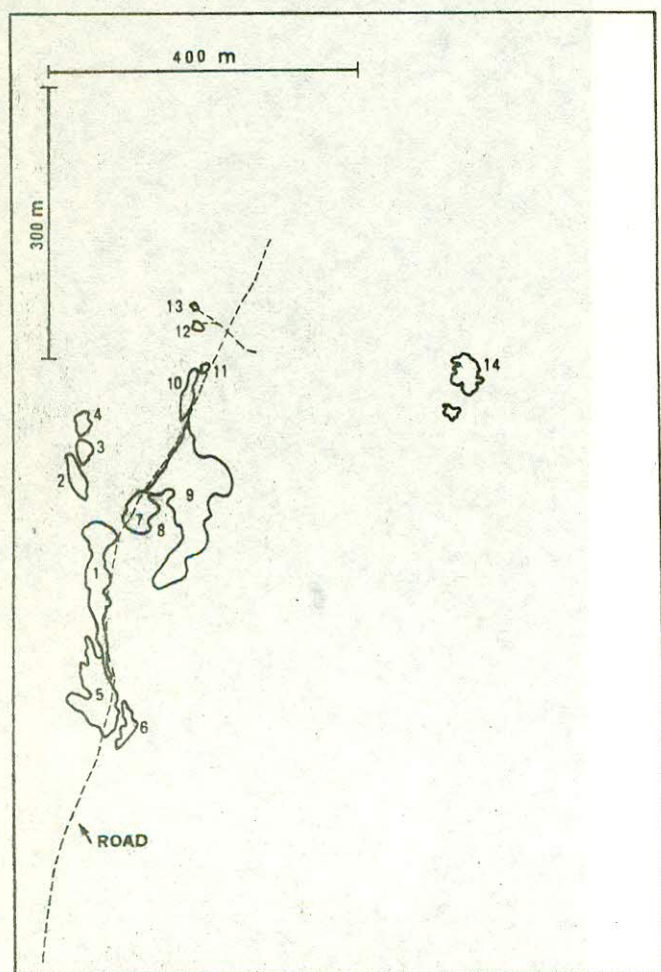


FIG. 6i. — Sketch at scale of 1968 image and signal amplitude level slices showing selected anomalously warm areas of uniform image density for which thermistor-derived temperature measurements at 0.5 m depth are given in text.



clastite ridges. It is likely that this group, although related to the same structure as the Hrafninnusker-Kaldsklofsfjöll fields, may be controlled by the northeast fissuring known to exist in this part of the area. Thus, three rows of solfatara fields within the Vestur-Reykjadalir are attributed to northeast-trending hidden faults.

#### Cost of infrared surveys in 1969

Airborne thermal infrared surveys may be conducted anywhere in the world at costs which are comparable to aerial photographic survey utilizing color films. With increasing availability of airborne thermal infrared scanners throughout the world, costs will become increasingly competitive with panchromatic aerial photographic surveys. The current high costs are controlled by four main factors: scarcity of trained operators for scanners (for optimum scanner operation during surveys, maintenance of scanner, and optimum processing of direct-record or videotape data), scarcity of scanners, mounting of scanner in survey aircraft, and high cost of sophisticated ancillary equipment for the scanner.

Thermal infrared scanners were originally developed for military reconnaissance applications, and ex-

cept for special circumstances, were in the past generally unavailable for non-military exploration and mapping applications. In the United States these limitations were partially eased in 1967, resulting in a marked increase in the use of airborne thermal infrared scanners in civil photogrammetry. Commercial firms, which had sold scanners to military users began marketing scanners for civilian purposes. Many firms offered survey services as well, and two firms: HRB-Singer, Inc., and Texas Instruments, Inc., had been conducting civil surveys for several years.

The University of Michigan's Institute of Science and Technology (IST), the United States Geological Survey (USGS), the Terrestrial Sciences Laboratory of U.S. Air Force Cambridge Research Laboratories (AFCRL), the U.S. National Aeronautics and Space Administration (NASA), and the U.S. Forest Service had also been conducting thermal infrared surveys for a number of years with their own scanners. Within the last two years, two commercial firms, Bendix and Daedalus Enterprises Inc., have been marketing scanners and conducting thermal infrared surveys. These two firms have also sold scanners to conventional aerial surveying firms. Several other countries (e.g., USSR, Sweden, Japan,

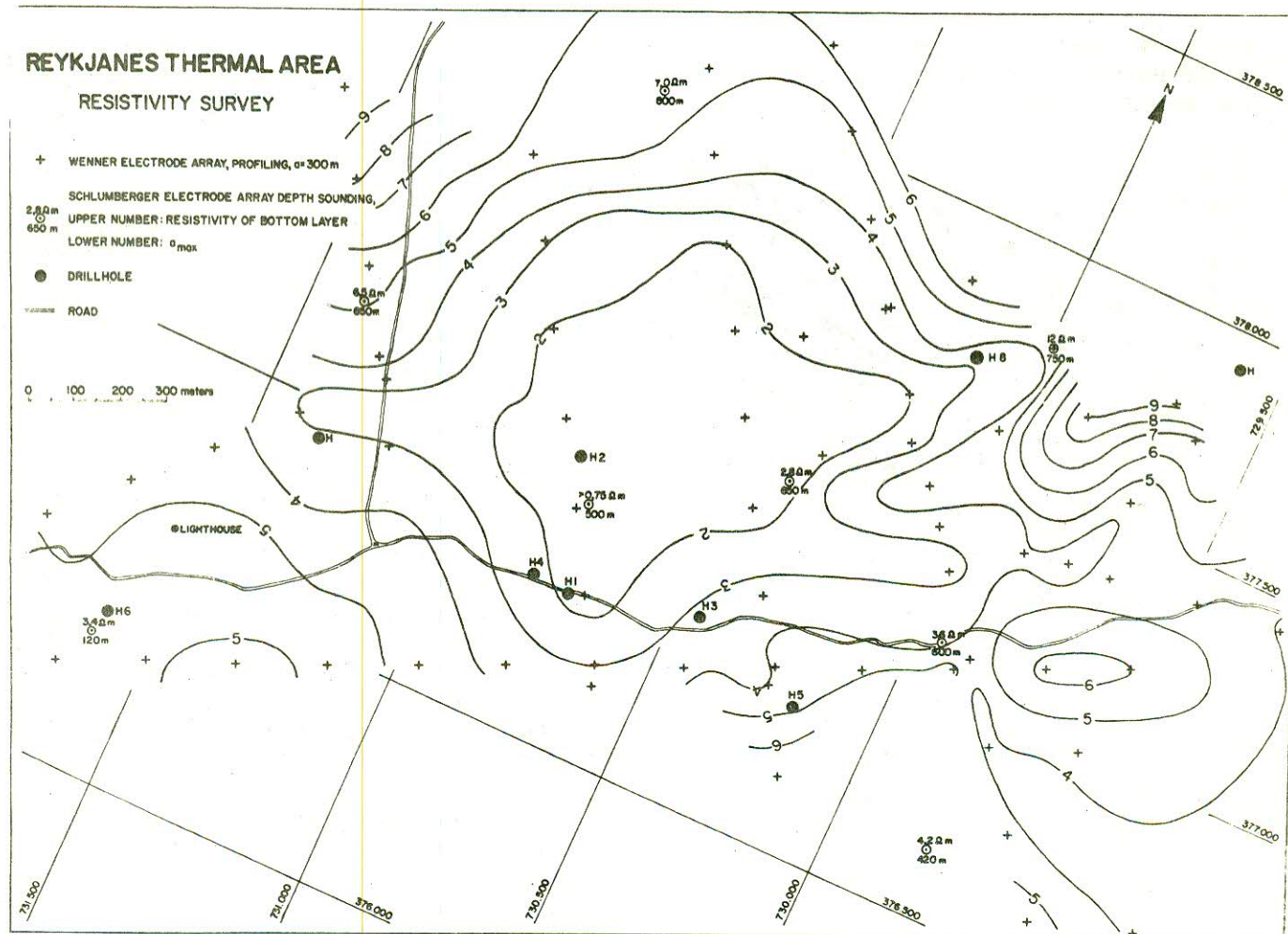


FIG. 7. — Resistivity map of the Reykjanes area.



etc.) have also developed and used scanners for airborne thermal infrared surveys of the earth's surface. Infrared scanners, suitable for use in light aircraft or helicopters are manufactured by two Swedish firms. AGA and Bofors; results of terrain surveys using these systems have recently been published (FAGERLUND ET AL. 1967).

Assuming chartered or contract surveys, the cost of any thermal infrared survey will vary depending on the following three factors: location of survey site(s), duration of survey, and type of aircraft used, the same three elements which affect cost of any airborne survey.

As an example, Table 2 shows the estimated daily cost for conducting thermal infrared surveys in North America in 1969.

Surveys at sites outside North America would generally involve the added cost of mobilization/demobilization expenses where equipment and personnel must be sent to the survey sites and the equipment (typically a cartographic camera mount) installed in another aircraft. Mobilization/demobilization costs in Australia, for example, would be approximately U.S. \$ 20,000. Survey costs as estimated in Table 2, do not take into account local variations and would be in addition to the mobilization/demobilization costs.

Commercial scanners and accessories may also be purchased or leased, hence, thermal infrared surveys may be accomplished by government agencies which do aerial surveying, commercial aerial surveying firms, etc.,

anywhere in the world. A scanner, however, is a sophisticated optical-mechanical-electronic device which is composed of five major elements: electronic amplifiers, optical elements, magnetic tape and/or film recorders, detector, and cryogenic system. Extensively trained personnel are required to maintain and operate the equipment for optimum airborne data recording. Post-survey processing of magnetic tape information can also be very sophisticated. Finally, experienced scientists are required to derive maximum information from thermal infrared imagery even in specific applications. The cost of data processing and analysis of the thermal infrared imagery must therefore be added to the total cost of conducting airborne thermal infrared surveys.

TABLE 2. — Example 1969 cost per day for survey in North America with a Cessna 195 <sup>(1)</sup>.

Scanner Lease	\$ 315
Operator Salary Expenses	180
Aircraft Costs for 6 Hours of Data Acquisition	660
Aircraft Costs for 2 Hours of Enroute and Turning Time	220
Aircraft Demurrage	220
Conversion of Taped Signals to Imagery (18 tapes)	720
Purchase of 18 Tapes	216
<b>TOTAL:</b>	<b>\$ 2,531</b>

Total Line-Kilometers <sup>(2)</sup>: 1450

Cost per Line-Kilometer: \$1.75

<sup>(1)</sup> Cost exclusive of ferry time from home airport to survey site (s). Compute ferry time at 130 knots with aircraft (Cessna 195) charges of \$220/ day and \$110/ flight hour. Assume a maximum of 8 hours ferry time per day. Add to aircraft ferry cost, scanner lease and operator daily rates for days in transit. All costs in U.S. dollars.

<sup>(2)</sup> Areal coverage of an airborne thermal infrared scanner is a function of scanner scan-angle (typically 72° to 120°) and survey altitude (distance between aircraft and terrain). For example, an aircraft flying at 1000 m above the terrain, with a scanner which scanned a total of 72° (36° each side of aircraft axis or nadir line on the ground) would cover 1600 m laterally or 800 m on each side of the nadir line.

## Conclusions

On the basis of the infrared surveys, which have been made over the Reykjanes and Torfajökull thermal areas in Iceland, it is concluded that this technique can give very useful information, particularly in areas which are poorly mapped by ground surveys. The pattern of anomalies can in places be related to known structural features and may also indicate previously unmapped structures which control the thermal activity. The imagery provides a map record at a specific time which can be compared with similar records made at other times to document changing patterns of thermal emission.

For the detection of abnormal heat flows the infrared technique is only moderately sensitive. The minimum heat flow anomalies that can with some confidence be recognized on the imagery, are an order of magnitude larger than the smallest abnormal heat flows

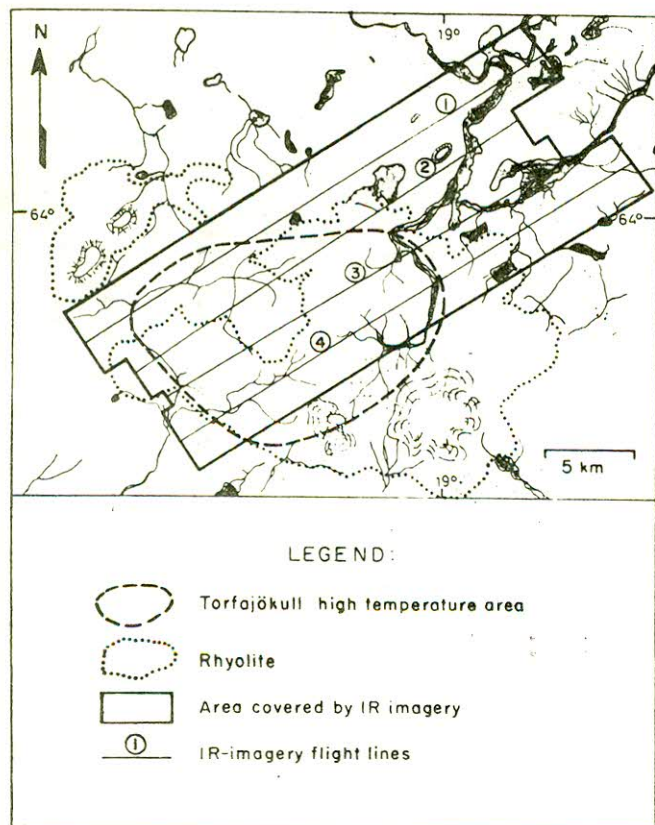


FIG. 8. — Infrared survey strips over the Torfajökull area.



which may be significant in geothermal exploration. But the level of detectability of anomalous heat flow by infrared imagery is greatly exceeded by the maximum heat flow density at thermal fields comparable to Reykjanes and Torfajökull. It is possible that, with a calibrated infrared scanner utilizing a DC restoration circuit, and a known energy transfer function, by means of a finer amplitude slicing of the low level anomalies, it may be possible to distinguish better between heretofore undetected low heat flow anomalies and the « noise » caused by sources other than variations in heat flow to the surface.

#### Acknowledgements

The work reported here was in part sponsored by the U.S. Geological Survey under Contract No. 14-08-001-11348 with the Icelandic National Energy Authority.

#### REFERENCES

- BJÖRNSSON S., ARNÓRSSON S., TÓMASSON J. 1970 — Exploration of the Reykjanes thermal brine area. *U.N. Symp. Development Utilization Geothermal Energy*, Pisa.
- BÖDVARSSON G., WALKER G. P. L. 1964 — Crustal drift in Iceland. *Geophys. J.*, 8, 285.
- DAWSON G. B. 1964 — The nature and assessment of heat flow from hydrothermal areas. *N.Z. J. Geol. Geophys.*, 7, 155.
- DECKER R. W., PECK D. L. 1967 — Infrared radiation from Alae lava lake, Hawaii. *Prof. Pap. U.S. Geol. Surv.*, 575-D, D169-D175.
- ENGLAND G., MORGAN J. O. 1965 — Quantitative airborne infrared mapping. *Proc. 3rd Symp. Remote Sensing Environment*, Ann Arbor, Mich., 681.
- FAGERLUND E., KLEMAN B., SELLIN L., SVENSSON H., MATSSON J. O., LINDQVIST S. 1967 — Infrarödtermografi, principer och naturgeografiska tillämpningar. *Svensk Geografisk Årsbok*, 43, 154.
- FRIEDMAN J. D., WILLIAMS R. S. Jr. 1968 — Infrared sensing of active geologic processes. *Proc. 5th Symp. on Remote Sensing of Environment*, Ann Arbor Mich., 787.
- FRIEDMAN J. D., WILLIAMS R. S. Jr., PALMASON G., MILLER C. F. 1969 — Infrared surveys in Iceland - Preliminary Report. *Prof. Pap. U.S. Geol. Surv.*, 650-C, p. C89-105.
- LEE W. H. K., UYEDA S. 1965 — Review of heat flow data. in: LEE W. H. K., ed. « *Terrestrial Heat Flow* », *Am. Geophys. Union. Geophys. Monograph* 8.
- ROBERTSON E. I., DAWSON G. B. 1964 — Geothermal heat flow through the soil at Wairakei. *N.Z.J. Geol. Geophys.*, 7, 134.
- SAEMUNDSSON K. 1969 — Infrared imagery of Torfajökull area. *National Energy Authority Rep.*, mimeographed, Reykjavik.
- WHITE D. E., MILLER L. D. 1969 — Calibration of geothermal infrared anomalies of low intensity in terms of heat flow, Yellowstone National Park (Abstract). *EOS. Trans. Amer. Geoph. Un.*, 50, 348.
- WILLIAMS R. S. Jr., FRIEDMAN J. D., THÓRARINSSON S., SIGURGEIRSSON T., PALMASON G. 1968 — Analysis of 1966 imagery of Surtsey, Iceland. in: *Surtsey Res. Soc. Progr. Rep.*, 4, 177.



FIG. 9. — Hydrothermal features in the Torfajökull area.



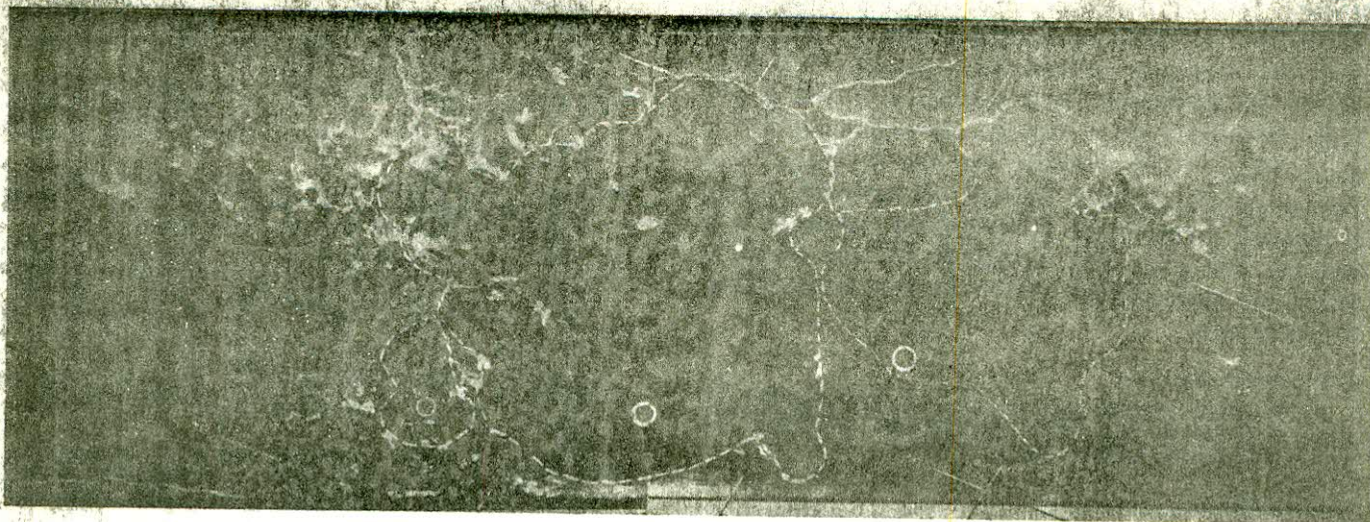


FIG. 10. — Infrared image strip of Hrafninnusker.

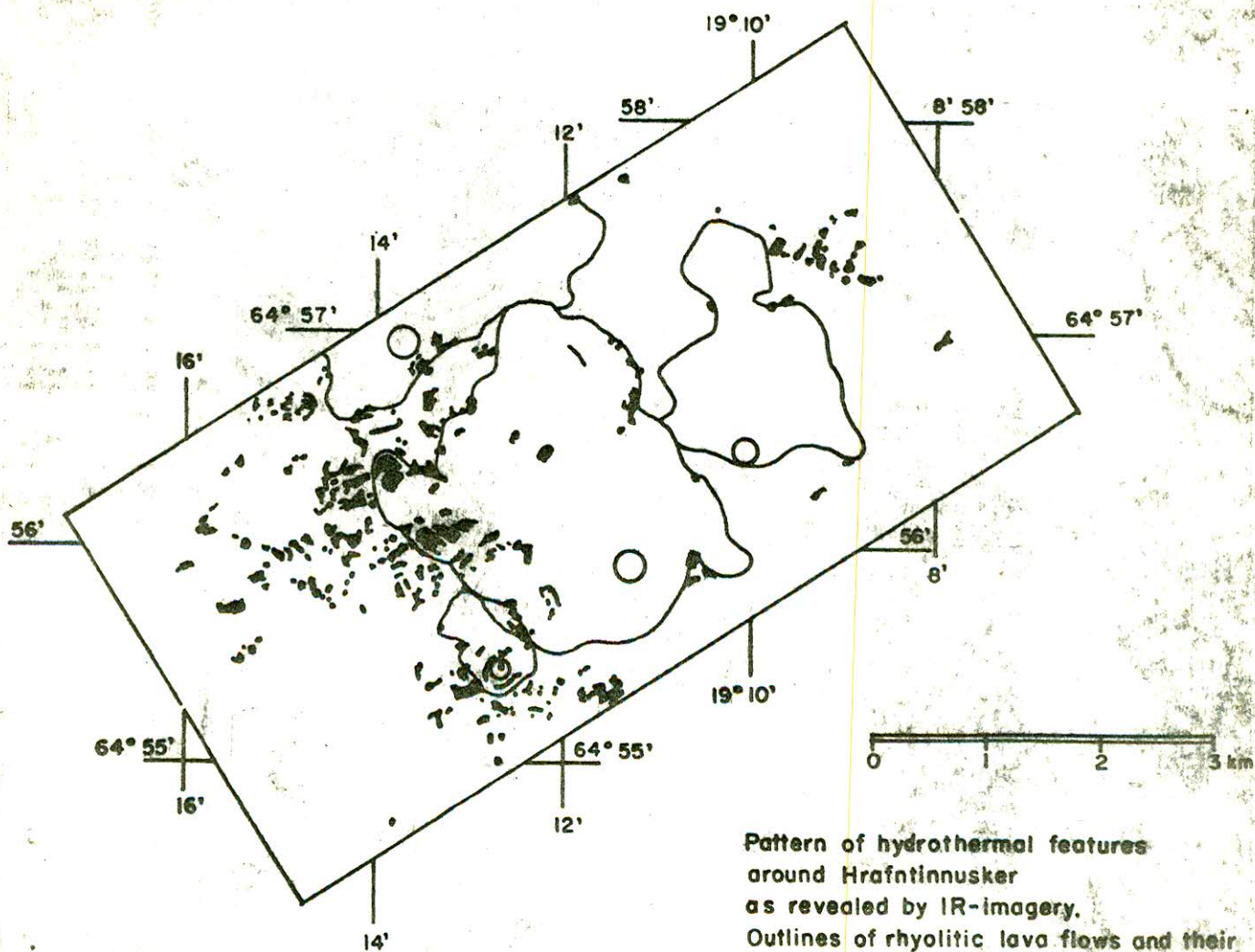


FIG. 11. — Map based on interpretation of infrared images of Hrafninnusker area.